

## Activities of Optical and Antibacterial Enhanced Microwave Assisted Zn<sub>2</sub>SnO<sub>4</sub> Nano Rods

Mohamed Haroon Basha A<sup>\*1</sup>, Steffi PF<sup>2</sup>, Thamilmaraiselvi B<sup>2</sup>, Bhuvaneshwari P<sup>2</sup>,  
Sangeetha K<sup>2</sup>, Mishel PF<sup>3</sup>

<sup>1</sup>Department of Physics, AMET DEEMED to be University, Chennai, India

<sup>2</sup>PG and Research Department of Microbiology, Cauvery College for Women  
(Autonomous), Trichirappalli.

<sup>3</sup>Research scholar, Department of Botany, Bharathidasan University, Trichy.

\*Corresponding author: harunbasha09@gmail.com

### Abstract

The nanorod Zinc stannate Zn<sub>2</sub>SnO<sub>4</sub> were studied and synthesized by ammonia with cubic spinel structure. The study of crystallography and optical properties were observed using X-ray diffraction and photoluminescence spectroscopy. The study of morphology of the nanoparticles was perceived using field emission scanning electron microscopy (FESEM). The effect of antibacterial of Zn<sub>2</sub>SnO<sub>4</sub> nanoparticle was tested against gram-positive and gram-negative and pathogenic bacteria have also studied.

Keywords: Zinc stannate; PL; nanoparticles; Nanoarchitectonics; antibacterial activity.

### Introduction

Zn<sub>2</sub>SnO<sub>4</sub>, an inverse structure of AB<sub>2</sub>O<sub>4</sub> compound has absorbed and unique properties interpreting it suitable for a wide range of applications such as transparent conducting electrodes, chemical sensors, photoelectrical devices, functional coatings and photocatalysts [1-3]. as a significant transparent semiconductor with wide band gap of 3.6 eV, The sample Zn<sub>2</sub>SnO<sub>4</sub> is known to have highly chemical sensitivity, high electrical conductivity and low visible absorption [4]. To understand the universal application of nanomaterials, the key point is to contrive simple and efficient methods for their preparation on a large scale at low cost. Different methods have employed to produce Zn<sub>2</sub>SnO<sub>4</sub> nanostructured i.e., mechano-chemical synthesis, thermal evaporation method by heating metal or metal oxide powder at high temperatures, simple co-precipitation method and hydrothermal synthesis [5-7].

In the food industry applications Metal oxide nanoparticles (NPs) are the most widely used antimicrobial agent [8]. The sample Zn<sub>2</sub>SnO<sub>4</sub> NPs displayed biocidal activity against a broad range of Gram-negative and Gram positive microorganisms [9]. The antimicrobial activity of

the sample  $Zn_2SnO_4$ NPs is based on the subsequent mechanisms: (a) release of  $Zn^{2+}/Sn^{2+}$  ions which bind to electron donor groups in molecules containing sulphur,nitrogen or oxygen, (b) DNA disruption replication and (c) oxidative stress through the catalysis of reactive oxygen species (ROS) formation [10]. ROS contain the most reactive hydroxyl radical (OH), the less toxic superoxide anion radical ( $\cdot O_2^-$ ) and hydrogen peroxide with a weaker oxidizer ( $H_2O_2$ ). Which damage DNA and cell membranes, etc., leading to cell death [11]. In the present work,  $Zn_2SnO_4$ nanorodswereprepared by a microwave assisted method. The structural properties of nano rods were characterized. The wide-range of optical behaviour of the sample  $Zn_2SnO_4$  nanorods and its antibacterial activity were also investigated.

## 2. Experimental methods

### 2.1. Synthesis

The consequent high purity chemicals Zinc (II) nitrate, Tin (II) chloride dihydrate and ammonia solution were used as precursors without further purification.

$Zn_2SnO_4$ nanoparticles were prepared in different ratio of Zn and Sn (2:1, 1:1 and 1:2) by Microwave-assisted precipitation method. Zinc (II) nitrate and Tin (II) chloride aqueous solutions (50 mL) were prepared and stirred for 1 h 20 min to get a homogeneous mixture. The solution of Ammonia was added to develop a white precipitate and stirred at the room temperature for 20 minutes. The solution was transmitted to poly propylene shielded autoclave bottle and the solution was irradiated by a microwave oven with 600 W Power for 10 min. After irradiation, the solution was cool down naturally to the room temperature. The precipitation was collected and washed several times with double distilled water and ethanol. Then the precipitate was dried at  $120^\circ C$ or 10 hs. at atmospheric condition and annealed at  $800^\circ C$  for 6 hours to obtain  $Zn_2SnO_4$ nanorods. The schematic diagram for the preparation of  $Zn_2SnO_4$ nanorodsis shown in Fig. 1.

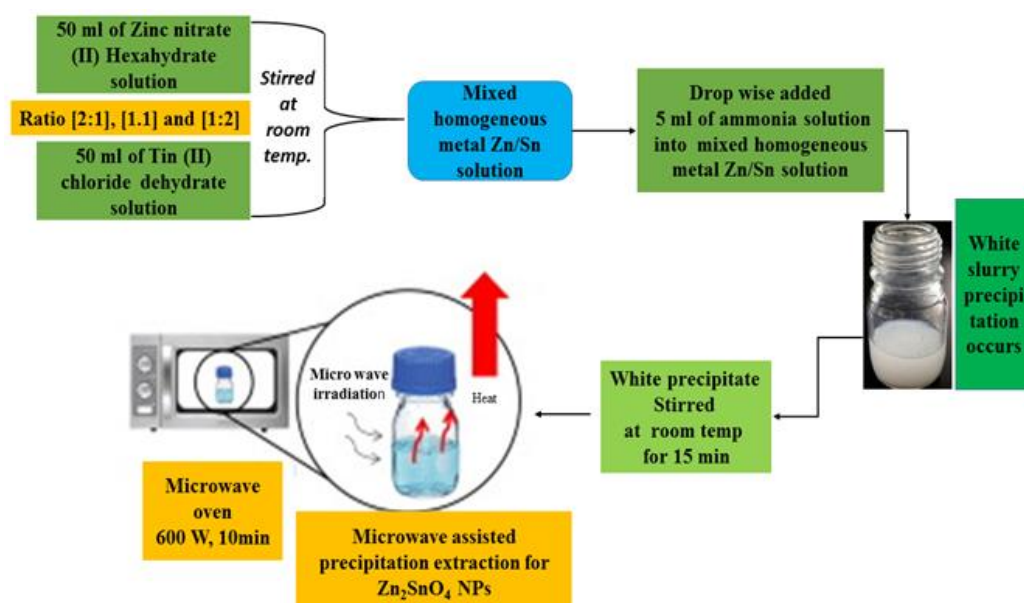


Fig. 1 Schematic diagram for the formation of  $Zn_2SnO_4$ nanorods.

## 2.2 Antibacterial assays

The antibacterial activity of microwave assisted Zn<sub>2</sub>SnO<sub>4</sub>nanorods was tested against *Streptococcus pneumoniae*, *Escherichia coli*, *Klebsiella pneumoniae* and *Shigella dysenteriae* bacterial strain were carried out in agar by well diffusion method. Tested the antibacterial activity at a concentration of 1 and 1.5 mg/ml of the sample Zn<sub>2</sub>SnO<sub>4</sub> nanorods dispersed in dimethylsulphoxide (DMSO). Inhibition zone levels (mm) was measured consequently after 25 hs at 36°C. For positive control, standard antibiotic Amoxicillin (30 µg disc) were used.

## 2.3 Characterization techniques

The structural properties of the sample Zn<sub>2</sub>SnO<sub>4</sub> were investigated and X-Ray diffraction patterns obtained using X'PERT PRO Panalytical Diffracto meter. The morphology of the sample Zn<sub>2</sub>SnO<sub>4</sub> nanorods was scrutinized by FESEM (Carl Zeiss Ultra 55) with EDAX (Inca). The functional groups were analysed by FT-IR spectra and documented by Perkin-Elmer spectrometer in the range of 450-4200 cm<sup>-1</sup>. And Photoluminescence spectra were taken JASCO spectro flurometer FP-8200 used to study the optical properties.

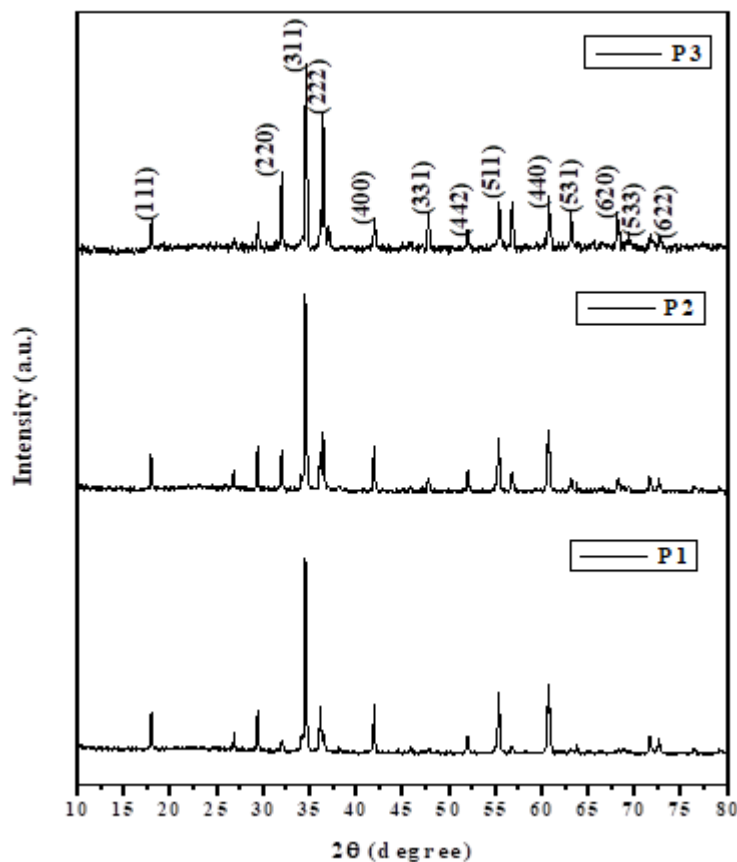
## 3 Results and discussion

### 3.1 X-ray diffraction patterns

The X-Ray diffraction patterns were obtained in reflection mode with Cu Kα (λ=1.5406 Å) radiation, in the 2θ range from 10° to 80° at room temperature. Figure 2 shows the X-ray diffractions patterns of the synthesized of the sample Zn<sub>2</sub>SnO<sub>4</sub> nanoparticles. The XRD patterns of the sample and the diffraction planes (111), (220), (311), (222), (400), (331), (442), (511), (440), (531), (620), (533) and (622), which exhibit spinel cubic structure. JCPDS #74-2184. The lattice constant a = 8.5714, 8.5781 and 8.5820 Å and volume V = 632.93, 632.19 and 629.86 Å<sup>3</sup> for P1, P2 and P3 respectively. The crystallite size of the Zn<sub>2</sub>SnO<sub>4</sub>nanorods are measured from Debye Scherrer's relation (eq.1) and the crystallite sizes were found to be 42nm for all the prepared samples (P1, P2 and P3) and the micro-strain (ε) (eq.2) was 0.00082 [12].

$$D = k\lambda/\beta \cos\theta \dots \dots \dots (1)$$

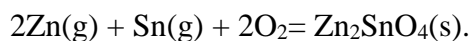
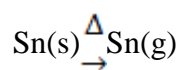
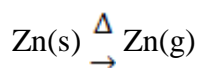
$$\varepsilon = \beta \cos\theta / 4 \dots \dots \dots (2)$$



**Figure 2 X-ray diffraction patterns of Zn<sub>2</sub>SnO<sub>4</sub> nanorods**

### 3.2 FESEM analysis

The surface morphology of microwave assisted sample Zn<sub>2</sub>SnO<sub>4</sub> nanorods were scrutinised through FESEM analysis is shown in Fig. 3(a-b). FESEM images clearly show the synthesized Zn<sub>2</sub>SnO<sub>4</sub> exhibits, rod like structure and average particle size in the nanoscale range. The nanorods formation may be due to two reasons such as crystal growth and crystal nucleation and direction. The growth mechanism of the sample Zn<sub>2</sub>SnO<sub>4</sub> nanorods can be described by chemical reactions and crystal growth, as follows: From the crystallization point of view, the synthesis of an oxide during an aqueous solution reaction is probable to experience a hydrolysis-condensation process. Growth of the sample Zn<sub>2</sub>SnO<sub>4</sub> nanorod arises from reaction.



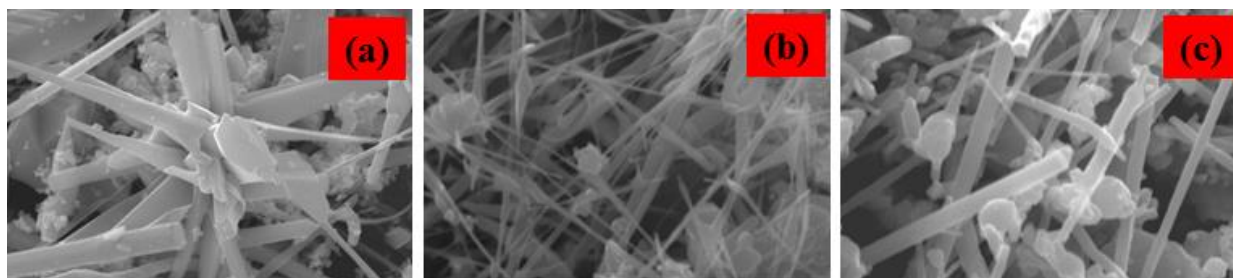


**Figure 3 (a-b) SEM images of Zn<sub>2</sub>SnO<sub>4</sub>nanorods**

### 3.3 Elemental compositions analysis

The elemental compositions of the Zn<sub>2</sub>SnO<sub>4</sub>nanorods are represented in Fig. 4 (a-c).From the EDAX spectra, the several area positions of the sample was chosen and scanning, the same Zn, Sn and O content was present. In the present work, the Zn, Sn and O elements of their atomic percentage are given Table 1. The concentration of Tin chloride during Synthesis is increasing and the oxygen percentage increased and Zinc and tin percentage decreased, this may be a local lattice strain.

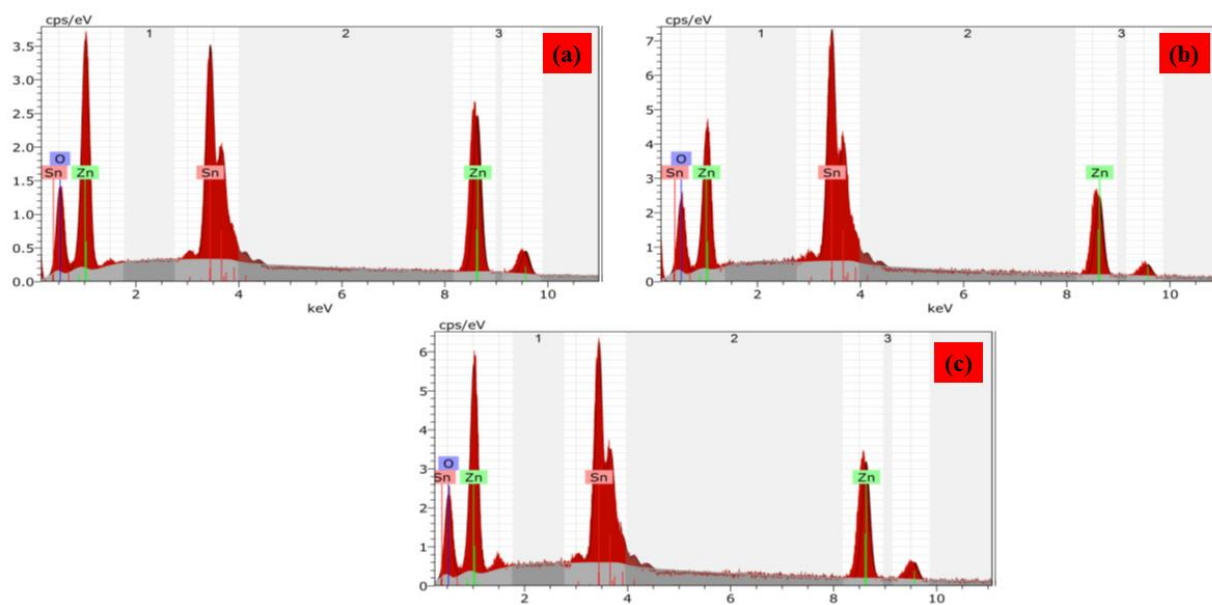


**Figure 4(a-c) EDAX spectra of Zn<sub>2</sub>SnO<sub>4</sub> NPs**

**Table 1 The Elemental composition percentage of Zn<sub>2</sub>SnO<sub>4</sub> NPs.**

Elements (atomic %)	P1	P2	P3
Tin	13.39	13.53	16.98
Zinc	25.21	24.69	18.26
oxygen	61.40	61.78	64.76

### 3.4 FTIR spectroscopic analysis

Figure 5 shows the FTIR spectra of various concentration of  $Zn_2SnO_4$  (2:1 (P1), 1:1(P2) and 1:2 (P3)) NPs. The many functional group of the  $Zn_2SnO_4$  samples are, O-H stretching at ( $3430, 3432$  and  $3416\text{ cm}^{-1}$ ) [13], C-H stretching at ( $2921$  and  $2924\text{ cm}^{-1}$ ) [14], C-H band at ( $2361$  and  $2336\text{ cm}^{-1}$ ), this can be absorb atmospheric C-O- O. The symmetric and asymmetric stretching C-O-O-group are found to be ( $1620, 1625$  and  $1632\text{ cm}^{-1}$ ) and ( $1469, 1416$  and  $1454\text{ cm}^{-1}$ ) [14] for P1, P2 and P3 samples. For  $Zn_2SnO_4$  NPs, The Zn-Sn-O bands found to be  $502, 475$  and  $460\text{ cm}^{-1}$  respectively, may be vibration of ZnO and  $SnO_2$  groups, and results formation of the Sn-O-Zn bonding in the  $Zn_2SnO_4$ [15].

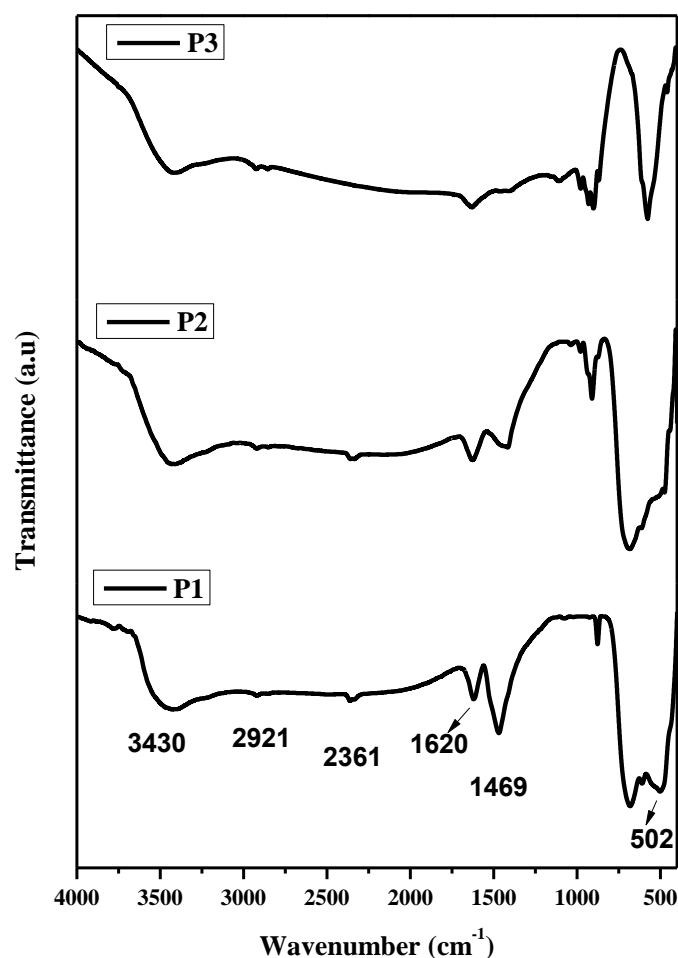
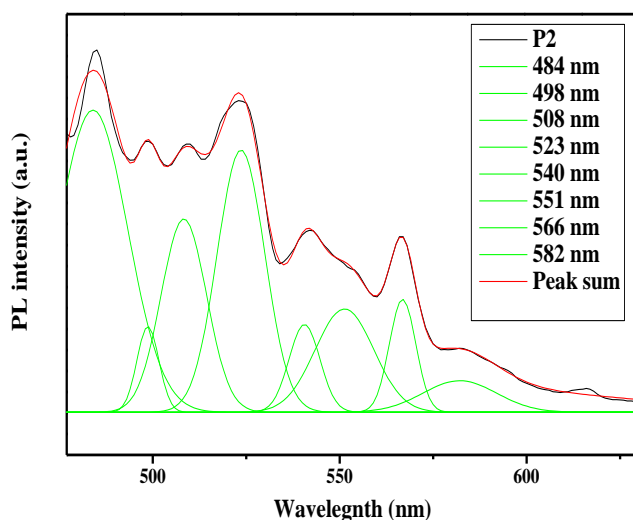
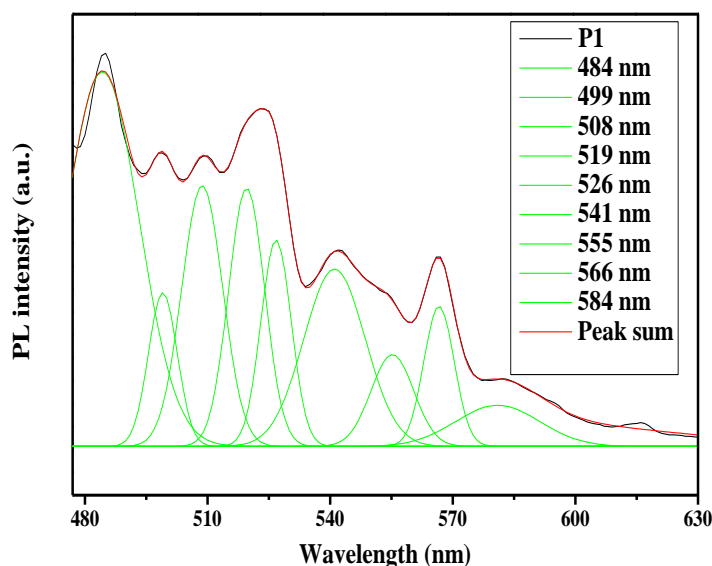


Figure 5 FTIR spectra of  $Zn_2SnO_4$  NPs

### 3.5 Photoluminescence spectroscopic studies

The photoluminescence spectra of microwave assisted  $Zn_2SnO_4$  nanorods is shown in Fig. 6 (P1-P3). The sample  $Zn_2SnO_4$  nanorods measured at the excitation wavelength of  $465\text{ nm}$ . The orange-yellow emission are located at ( $484, 499, 508, 519, 526, 541, 555, 566,$  and  $584\text{ nm}$ ), ( $484, 498, 508, 523, 540, 550, 565,$  and  $580\text{ nm}$ ) and ( $483, 495, 507, 520, 525, 542, 556,$

568, and 580 nm) for P1, P2 and P3 respectively. The blue-green emission found to be (485-490 nm) for all Zn<sub>2</sub>SnO<sub>4</sub> nanorods, which is attributed to oxygen vacancies [16, 17]. The green emission observed at (510-550 nm) for P1, P2 and P3 samples respectively, usually the oxygen vacancies existing in ZnSnO<sub>4</sub> [18,19]. The yellow-orange emission centered at (567 and 580 nm) for Zn<sub>2</sub>SnO<sub>4</sub> nanorods respectively, due to the interaction between oxygen vacancies, sum of meta stable energy levels in the band gap of the as-synthesized Zn<sub>2</sub>SnO<sub>4</sub> NPs. For the sample P3, green emission values (580 nm) which is increased as compared with P2 (584 nm) and the sample P1 (586 nm) for Zn<sub>2</sub>SnO<sub>4</sub> respectively. From the optoelectronic application generally depends on decrease in defect level, which is mainly influenced via electron phonon coupling interaction. In this work, the P3 emission decreased as compared with P1 and the sample P2, this results sustenance for the future development of optoelectronic application.



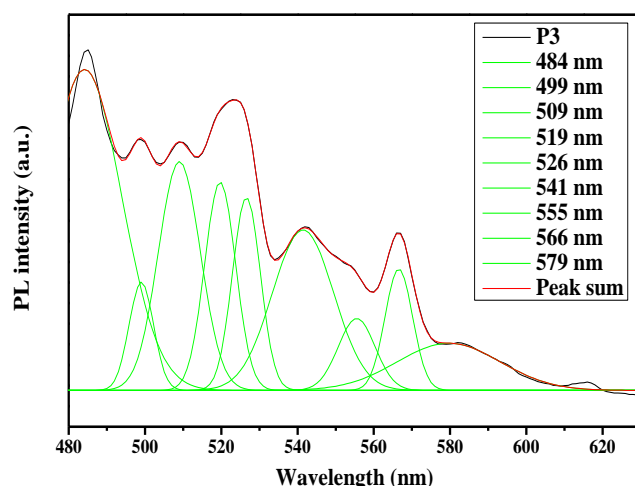


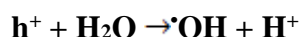
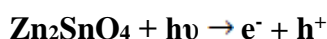
**Figure 6 PL spectra of Zn<sub>2</sub>SnO<sub>4</sub> NPs**

### 3.7 Antibacterial activity

Figure 7 (a-b) shows antibacterial activity of Microwave assisted Zn<sub>2</sub>SnO<sub>4</sub> NP tested against *Streptococcus pneumoniae*, *Escherichia coli*, *Klebsiella pneumoniae* and *Shigella dysenteriae* bacterial strains to determine by the well diffusion method. The Amoxicillin and the sample Zn<sub>2</sub>SnO<sub>4</sub>NPs show the antibacterial activity and the inhibition zone and specifies the biocidal action.

The antibacterial activity generally depends on production of reactive oxygen species (ROS) [21-23]. This ROS on the surface of these nanoparticles in light causes oxidative stress in microbial cells membrane, ultimately leading to the death of the cells.

The production of ROS can be given



The Zn<sub>2</sub>SnO<sub>4</sub> nanorods through defects can be activated, both UV and visible light, electron-hole pairs can be created. The holes fragmented H<sub>2</sub>O molecules hooked on OH<sup>-</sup> and H<sup>+</sup>. Dissolved (O<sub>2</sub>) can be converted to (·O<sub>2</sub><sup>-</sup>) radical anions. The (·O<sub>2</sub><sup>-</sup>) superoxide radical anions in turn react with H<sup>+</sup> to create HO<sub>2</sub>· radicals. The hydrogen ions (H<sup>+</sup>) react with HO<sub>2</sub>· to produce molecules of H<sub>2</sub>O<sub>2</sub>. The H<sub>2</sub>O<sub>2</sub> production be able to penetrate the cell membrane and finally bacteria death occur [24]. On other hand, Zn<sup>2+</sup>/Sn<sup>2+</sup> ions are released by Zn<sub>2</sub>SnO<sub>4</sub> comes into contact with microbial cell membranes, the cell membranes with (-) charge and

## Activities of Optical and Antibacterial Enhanced Microwave Assisted Zn<sub>2</sub>SnO<sub>4</sub> Nano Rods

Zn<sup>2+</sup>/Sn<sup>2+</sup> ions with (+) charge mutually attract. The metal ions Zn<sup>2+</sup>/Sn<sup>2+</sup> are penetrates on the cell membrane and reacted by sulfydryl groups inside the cell membrane. As a result, the damaged microbe synthetase activity and cellslosing their ability of cell division, which leads to the cell death of the bacteria.

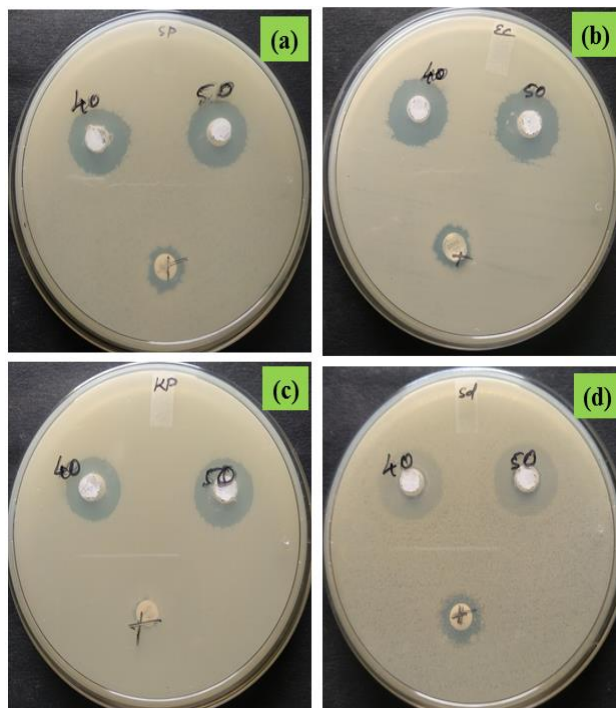


Figure 7 Progressive antibacterial activity of G+ and G- bacteria

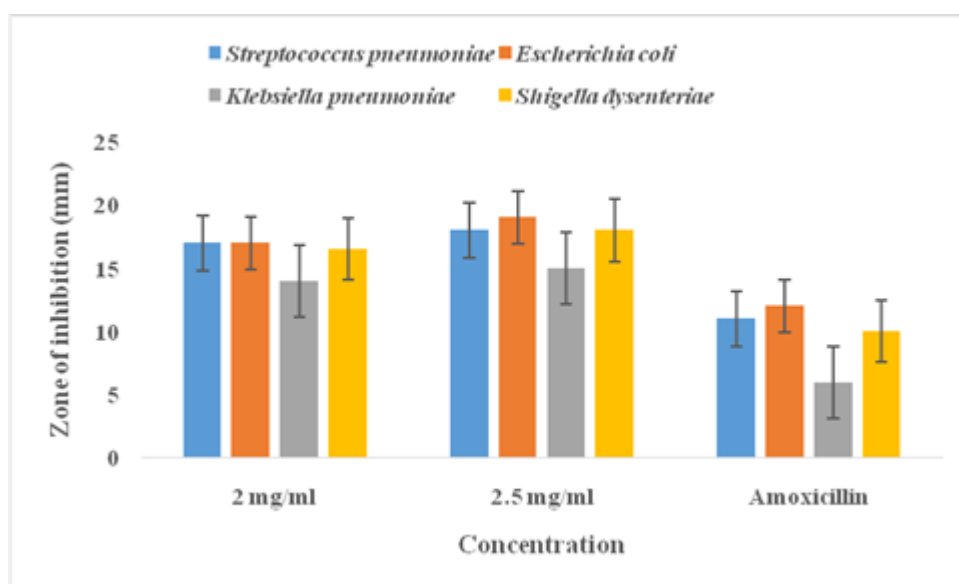


Figure 8 The Zone of inhibition for various bacterial strain treated with Zn<sub>2</sub>SnO<sub>4</sub> NPs

## 4 Conclusions

In summary, the Zn<sub>2</sub>SnO<sub>4</sub> nanorods were prepared through facile hydrothermal method using microwave oven. The XRD patterns showed that synthesized nanorods shows spinel cubic structure. Nanorod like morphology and chemical composition were observed through FESEM and EDAX spectra. In case of FT-IR spectra, the (Zn-Sn-O) stretching bands were observed at 505, 470 and 460 cm<sup>-1</sup> for all Zn<sub>2</sub>SnO<sub>4</sub> NPs. PL spectra, due to strong support for the potential development of wide-range of optical and electrical device application, the Zn<sub>2</sub>SnO<sub>4</sub> (P3) emission decreased as compared with P1 and P2, the nanorods(Zn<sub>2</sub>SnO<sub>4</sub>) showed the antibacterial activity and the inhibition zone which indicates the biocidal action of Zn<sub>2</sub>SnO<sub>4</sub> nanorods. These materials were used as a bactericidal agent to control and prevent and the spread and persistence of infectious diseases.

## Reference

1. Ali, Monaam Ben, Fatiha Barka-Bouaifel, Habib Elhouichet, Brigitte Sieber, Ahmed Addad, Luc Boussekey, Mokhtar Férid, and Rabah Boukherroub. "Hydrothermal synthesis, phase structure, optical and photocatalytic properties of Zn<sub>2</sub>SnO<sub>4</sub> nanoparticles." *Journal of colloid and interface science* 457 (2015): 360-369.
2. Zeng, Jia, MuDi Xin, KunWei Li, Hao Wang, Hui Yan, and WenJun Zhang. "Transformation process and photocatalytic activities of hydrothermally synthesized Zn<sub>2</sub>SnO<sub>4</sub> nanocrystals." *The Journal of Physical Chemistry C* 112, no. 11 (2008): 4159-4167.
3. Wang, W-W., Y-J. Zhu, and L-X. Yang. "ZnO–SnO<sub>2</sub> hollow spheres and hierarchical nanosheets: hydrothermal preparation, formation mechanism, and photocatalytic properties." *Advanced Functional Materials* 17, no. 1 (2007): 59-64.
4. Fu, Gang, Huan Chen, Zhexiong Chen, Jinxiu Zhang, and Heinz Kohler. "Humidity sensitive characteristics of Zn<sub>2</sub>SnO<sub>4</sub>–LiZnVO<sub>4</sub> thick films prepared by the sol–gel method." *Sensors and Actuators B: Chemical* 81, no. 2-3 (2002): 308-312.
5. Šepelák, Vladimír, Sebastian M. Becker, Ingo Bergmann, Sylvio Indris, Marco Scheuermann, Armin Feldhoff, Christian Kübel et al. "Nonequilibrium structure of Zn<sub>2</sub>SnO<sub>4</sub> spinel nanoparticles." *Journal of Materials Chemistry* 22, no. 7 (2012): 3117-3126.
6. Jaculine, M. Mary, C. Justin Raj, and S. Jerome Das. "Hydrothermal synthesis of highly crystalline Zn<sub>2</sub>SnO<sub>4</sub> nanoflowers and their optical properties." *Journal of Alloys and Compounds* 577 (2013): 131-137.
7. Zhao, Yang, Ying Huang, Qiufen Wang, Ke Wang, Meng Zong, Lei Wang, Wei Zhang, and Xu Sun. "Preparation of hollow Zn<sub>2</sub>SnO<sub>4</sub> boxes for advanced lithium-ion batteries." *Rsc Advances* 3, no. 34 (2013): 14480-14485.
8. Raja, A., S. Ashokkumar, R. Pavithra Marthandam, J. Jayachandiran, Chandra Prasad Khatiwada, K. Kaviyarasu, R. Ganapathi Raman, and M. Swaminathan. "Eco-friendly preparation of zinc oxide nanoparticles using *Tabernaemontana divaricata* and its photocatalytic and antimicrobial activity." *Journal of Photochemistry and Photobiology B: Biology* 181 (2018): 53-58.
9. Dinesh, S., S. Barathan, V. K. Premkumar, G. Sivakumar, and N. Anandan. "Hydrothermal synthesis of zinc stannate (Zn<sub>2</sub>SnO<sub>4</sub>) nanoparticles and its application

- towards photocatalytic and antibacterial activity." *Journal of Materials Science: Materials in Electronics* 27, no. 9 (2016): 9668-9675.
10. Hameed, Abdulrahman Syedahamed Haja, Chandrasekaran Karthikeyan, Abdulazees Parveez Ahamed, Nooruddin Thajuddin, Naiyf S. Alharbi, Sulaiman Ali Alharbi, and Ganasan Ravi. "In vitro antibacterial activity of ZnO and Nd doped ZnO nanoparticles against ESBL producing Escherichia coli and Klebsiella pneumoniae." *Scientific reports* 6 (2016): 24312.
  11. Foster, Howard A., Iram B. Ditta, Sajnu Varghese, and Alex Steele. "Photocatalytic disinfection using titanium dioxide: spectrum and mechanism of antimicrobial activity." *Applied microbiology and biotechnology* 90, no. 6 (2011): 1847-1868.
  12. Hankare, P. P., P. A. Chate, D. J. Sathe, P. A. Chavan, and V. M. Bhuse. "Effect of thermal annealing on properties of zinc selenide thin films deposited by chemical bath deposition." *Journal of Materials Science: Materials in Electronics* 20, no. 4 (2009): 374-379.
  13. Y. Wang, X. Liao, Z. Huang, G. Yin, J. Gu, Y. Yao, *Colloids Surf. A* 372, 165 (2010)
  14. Vijayaprasath, G., P. Soundarrajan, and G. Ravi. "The point defects induced ferromagnetism in ZnO semiconductor by terbium doping via co-precipitation method." *Journal of Materials Science: Materials in Electronics* 29, no. 14 (2018): 11892-11900.
  15. Jeronsia, J. Emima, L. Allwin Joseph, M. Mary Jacqueline, P. Annie Vinosha, and S. Jerome Das. "Hydrothermal synthesis of zinc stannate nanoparticles for antibacterial applications." *Journal of Taibah University for Science* 10, no. 4 (2016): 601-606.
  16. Wang, J. X., S. S. Xie, Y. Gao, X. Q. Yan, D. F. Liu, H. J. Yuan, Z. P. Zhou et al. "Growth and characterization of axially periodic Zn<sub>2</sub>SnO<sub>4</sub> (ZTO) nanostructures." *Journal of Crystal Growth* 267, no. 1-2 (2004): 177-183.
  17. Wang, J. X., S. S. Xie, H. J. Yuan, X. Q. Yan, D. F. Liu, Y. Gao, Z. P. Zhou et al. "Synthesis, structure, and photoluminescence of Zn<sub>2</sub>SnO<sub>4</sub> single-crystal nanobelts and nanorings." *Solid state communications* 131, no. 7 (2004): 435-440.
  18. Wang, Jianxiong, Xiao Wei Sun, Shishen Xie, Weiya Zhou, and Yi Yang. "Single-crystal and twinned Zn<sub>2</sub>SnO<sub>4</sub> nanowires with axial periodical structures." *Crystal Growth and Design* 8, no. 2 (2007): 707-710.
  19. Kim, Han Sung, Seon Oh Hwang, Yoon Myung, Jeunghee Park, Seung Yong Bae, and Jae Pyoung Ahn. "Three-dimensional structure of helical and zigzagged nanowires using electron tomography." *Nano letters* 8, no. 2 (2008): 551-557.
  20. Zhao, Jian-Wei, Li-Rong Qin, and Li-De Zhang. "Single-crystalline Zn<sub>2</sub>SnO<sub>4</sub> hexangular microprisms: Fabrication, characterization and optical properties." *Solid state communications* 141, no. 12 (2007): 663-666.
  21. Li, Qilin, Shaily Mahendra, Delina Y. Lyon, Lena Brunet, Michael V. Liga, Dong Li, and Pedro JJ Alvarez. "Antimicrobial nanomaterials for water disinfection and microbial control: potential applications and implications." *Water research* 42, no. 18 (2008): 4591-4602.
  22. Foster, Howard A., Iram B. Ditta, Sajnu Varghese, and Alex Steele. "Photocatalytic disinfection using titanium dioxide: spectrum and mechanism of antimicrobial activity." *Applied microbiology and biotechnology* 90, no. 6 (2011): 1847-1868.

23. Wilson, Martin R., Janet H. Lightbody, Ken Donaldson, Jill Sales, and Vicki Stone. "Interactions between ultrafine particles and transition metals in vivo and in vitro." *Toxicology and applied pharmacology* 184, no. 3 (2002): 172-179.
24. Fang, Ming, Ji-Hua Chen, Xiu-Li Xu, Pei-Hong Yang, and Hartmut F. Hildebrand. "Antibacterial activities of inorganic agents on six bacteria associated with oral infections by two susceptibility tests." *International Journal of Antimicrobial Agents* 27, no. 6 (2006): 513-517.